QC929
.A8
T68
no. 8

U. S. DEPARTMENT OF AGRICULTURE

FOREST SERVICE

ALTA AVALANCHE STUDY CENTER

WASATCH NATIONAL FOREST

Translation No. 8

RMRS Library
USDA Forest Service
FEB 2 2 2007
240 W Prospect Rd
Fort Collins CO 80526

# Stability of Snow Slabs

By

C. JACCARD
Swiss Federal Institute for Snow and Avalanche Research
Weissfluhjoch, Davos

Translated by Angie Thacker

September 1968

# STABILITY OF SNOW SLABS

C. JACCARD

Swiss Federal Institute for snow and avalanche research

Weissfluhjoch, Davos
(Translated by Angie Thacker, Alta Avalanche Study Center)

## ABSTRACT

The comparison of stresses in the weakest layer with the corresponding critical curve in the mohr plane leads to a definition of primary stability. Investigation of this definition as a function of slope angle and distributed load, shows it to be in certain cases, independent of load.

Secondary stability characterizes the absence of sensitivity to perturbations, especially to a localized rupture of the critical layer. Here, consideration is given to different shapes of the fracture zone and also the influence of a vertical concentrated force applied to the surface.

## 1. INTRODUCTION

The rupture of snow slabs seems to be a principal cause of avalanche release and may occur any time during the winter season so long as the conditions of snow, temperature, wind, and topography are favorable. When the temperature is sufficiently high, avalanches may release alternatively in a pear-shaped fashion; however, in most cases this does not shift large masses. It is therefore of particular interest to study the stability of slabs.

A slab is in equilibrium when its weight is balanced by the forces which act around its top, side, bottom and base. The first question that comes to mind is the relative importance of the basal forces in relation to the non-basal forces. This depends first of all on the ratio between the dimensions of the slab parallel to the slope and its thickness. No detailed statistics exist on this ratio, however some indication may be deduced from the 1959-1963 reports of the

Swiss Federal Institute. The histogram of Fig. 1 shows that the distribution of the width of snow slabs released in the region of the Parsenn has a net maximum between 20 and 40 m. The second maximum for the slabs larger than 100 meters is probably not realistic since these large slabs are often composed of several smaller slabs. Slab thickness is generally unknown, but it may be estimated to average about 0.5 meters. Thus the ratio of width to thickness usually exceeds 40. In ten cases where the stratigraphic profile of the slab was actualiy examined, this ratio was always higher than 50. In addition, the relative importance of the basal force depends on the snow strength at the base in comparison to snow strength throughout the thickness of the slab; here also, numerical data is rare. Rammsonde measurements in certain instances show ratios of up to 5 to 1 between the strength of the base and the slab profile.

Thus it seems that in the majority of cases basal conditions determine stability, the periphery only intervening when a critical state exists at the base or in certain cases conditioned by the terrain (couloirs). Therefore the following analysis will be limited to slabs which extend infinitely in two dimensions and fail only along the basal plane.

## 2. STATIC CONDITIONS

Let us consider an infinite slab of thickness, h, sloped at an angle, $\psi$. We adopt a system of rectangular coordinates with axes x, y, and z (see Fig.2). This is the case of plane stress studied by Haefeli (1942) and is defined in part by the following equations

$$\frac{\partial \sigma_y}{\partial y} = \gamma \cos\psi, \quad \frac{\partial \sigma_x}{\partial x} = 0, \quad \frac{\partial \tau_{xy}}{\partial y} = \gamma \sin\psi \tag{1}$$

where $\gamma$ is the density of the snow.

Assume that the velocity components, $V_x$, $V_y$, and $V_z$ depend on stress according to an extension of the plasticity equations of Lame

$$\frac{\partial V_x}{\partial x} = a\left[\sigma_x - \frac{1}{m}(\sigma_y + \sigma_z)\right]$$

$$\frac{\partial V_x}{\partial y} + \frac{\partial V_y}{\partial x} = 2a\left(1 + \frac{1}{m}\right)\tau_{xy} \qquad (2)$$

with permutations of the indexes for the other components. In Equation (2), $m$ is the plastic poisson number and $a$ represents a coefficient of viscosity. It is obvious that this representation can give only a first approximation since there is no guarantee that stress is a linear function of velocity. Also, $m$ does not have the same value in tension as it has in compression. Thus we must be careful not to attribute too much precision to the ensuing analysis.

For the case of plane stress on an infinitely extended slope, the velocity gradients in the x and z directions vanish

$$\frac{\partial V_x}{\partial x} = 0 \quad ; \quad \sigma_x - \frac{1}{m}(\sigma_y + \sigma_z) = 0$$

$$\frac{\partial V_z}{\partial z} = 0 \quad ; \quad \sigma_z - \frac{1}{m}(\sigma_x + \sigma_y) = 0 \qquad (3)$$

Thus the following expressions are obtained

$$\sigma_y = \cos\psi \int_0^y \gamma\, dy \quad , \quad \tau_{xy} = \sin\psi \int_0^y \gamma\, dy$$

$$\sigma_x = \sigma_z = \frac{\sigma_y}{m-1} = \frac{\cos\psi}{m-1} \int_0^y \gamma\, dy \qquad (4)$$

The local angle of creep is defined as

$$\tan\beta = \frac{\partial V_y}{\partial y} \Big/ \frac{\partial V_x}{\partial y} \qquad (5)$$

Because the derivatives along x disappear, this is equal to

$$\frac{m-2}{2(m-1)} \cot\psi \qquad (6)$$

The principal stresses are

$$\sigma_{1,2} = \left[ \frac{m}{2m-2} \pm \sqrt{\left(\frac{m-2}{2m-2}\right)^2 + \tan^2\psi} \right] \cos\psi \int_0^y \gamma \, dy \tag{7}$$

and are at an angle, $\alpha$ , to the coordinates, given by

$$\tan 2\alpha = \frac{2(m-1)}{(m-2)} \tan\psi \tag{8}$$

For each depth, y, between 0 and h, $\sigma_1$ and $\sigma_2$ determine a circle, $C_m$, in the Mohr-plane (Fig. 3). A curve, $C_r$, can also be constructed to represent the strength of the snow at a depth, y. The usual criterium of stability is that this latter curve does not touch the Mohr's circle. This is called the "criterium of primary stability" as opposed to other kinds of stability which we will consider later on.

If an overload is applied to the snow cover, or the slope angle increases, the circle, $C_m$, is enlarged and displaced. It is also possible that the strength curve may shift due to a change in the properties of the material (e.g. a temperature rise or a metamorphism of the snow). In either case, the first layer for which the Mohr's circle touches the strength curve, is defined to be a <u>critical layer.</u>

## 3. VARIATION OF PRIMARY STABILITY

For abbreviation, let us call

$$g(y) = \int_0^y \gamma \, dy \tag{9}$$

The strength curve may be approximated by a straight line inclined to the $\sigma$-axis at an angle, $\omega$ . This line cuts the $\tau$ - axis at $\tau_c$ (Fig. 3). If a line tangent to the Mohr's circle, inclined to the $\sigma$ - axis at an angle, $\omega$ ,

intersects the $\tau$ - axis at $\tau_1$ , the criteria of primary stability is simply

$$\tau_1 < \tau_c \tag{10}$$

$\tau_1$ , is found from

$$\tau_1 = \left[ \frac{(M^2 + \tan^2\psi)^{1/2}}{\cos\omega} - (1 - M)\tan\psi \right] g \cos\psi \tag{11}$$

where M, the "compressibility," is defined as

$$M = \frac{m-2}{2m-2}$$

$$0 \leq M \leq 1/2 \tag{12}$$

Let us first consider homogeneous slabs of equal thickness and examine the variation of stability with slope angle. In Fig. 4, $\tau_1/g$ is shown as a function of $\psi$ for different values of the parameter $\omega$ , and for two extreme values of

$$m = \infty \quad , \quad m = 2$$

It can be observed that for slabs of equal thickness, steeper slopes are more critical. However, let us next consider the case of slab thickness varying with the slope angle. This situation is observed when snow falls with little wind. Then, $g$ must be replaced by $g_0 \cos\psi$ , where $g_0$ is the slab thickness on level terrain. As shown in Fig. 5, the shape of the curves change. $\tau_1$ is maximum between $35^\circ$ and $50^\circ$ for $m = \infty$ ; and is maximum between $45^\circ$ and $65^\circ$ for $m = 2$ . This indicates that if $\tau_1$ increases progressively up to $\tau_c$ (a continuous fall of snow), slopes of about $45^\circ$ rupture before the steeper slopes.

If only slopes of practical interest are considered, say below $50^\circ$, primary stability is assured for all slopes if the load, $g$ , is less than 80% of $\tau_c$ (60% with constant snow height).

Since stability varies as $g$ changes, it is possible to define a limiting slope which is "absolutely stable" independent of an increase in $g$ . In fact, it can be seen in Fig. 4 and Fig. 5 that if $m$ is small enough, $\tau_1$ can be less

than zero. Since $\tau_c > 0$ , Equation 10 is satisfied under this condition for all values of $g$ . The slope angle, $\psi_1$ , of "primary absolute stability" is found by setting $\tau_1 = 0$ in Equation (10)

$$\tan^2 \psi_1 = (1 - M)^2 \sin^2 \omega - M^2 \qquad (13)$$

A plot of Equation (13) is shown in Fig. 6. $\psi_1$ exists only if $M$ is sufficiently small, i.e. if the snow is sufficiently incompressible, and increases in a uniform manner with the parameter, $\omega$ .

If stability is not initially absolute, the situation may improve according to particular conditions. A settling of the snow causes a decrease in $m$ and consequently a decrease in $M$ . According to Fig. 7, this results in a decrease in $\tau_1$ and therefore an increase in stability. This effect becomes greater as the slope angle decreases and $\omega$ increases.

## 4. SECONDARY STABILITY

Secondary stability is only assured for a slab which has primary stability and which remains stable if it is submitted to a perturbation. The perturbation may be, for example, a local break in the critical layer. The forces sustained by the critical layer are transferred to neighboring zones with a marked maximum along the boundaries of the slab and a possible propagation of the fracture.

Two extreme cases are observed for the configuration of fracture lines: a circular pattern and an extended horizontal pattern. The first case is analogous to considering the stress on a cylinder of radius, $r_0$ , and thickness $y$ . The exact solution of this problem is very complicated and depends on the visco-elastic properties of all the layers in the slab.

We limit our analysis to the simple case which rests on the following hypotheses. First, the component of the weight of the cylinder which is normal to

the slope is always balanced (even after failure) by the supporting base, only the tangential components are redistributed along the boundary; and second, the stresses created by a concentrated force are propagated through the snow according to an attenuation function which can be expressed as a power series in $\frac{1}{r}$, where $r$ is the distance to the point of application of the concentrated force. If $r$ is relatively large, the term of the series with the smallest exponent, $k$, is the dominating term and the other terms can be disregarded. Then, the increase in stress caused by a concentrated force is

$$\Delta\tau = \frac{T(k-2)}{2\pi r_0^2}\left(\frac{r_0}{r}\right)^k \tag{14}$$

and according to the first hypothesis

$$T = g\pi r_0^2 \sin\psi = \pi r_0^2 \tau \tag{15}$$

The stress change at $r = r_0$ becomes

$$\Delta\tau_{r=r_0} = \tau\left(\frac{k}{2} - 1\right) \tag{16}$$

and the total stress at $r = r_0$ is now

$$\tau + \Delta\tau = \frac{k}{2}\tau \tag{17}$$

The exponent, $k$ is determined by the viscosity of the layer. When the viscosity is large, the forces are more concentrated, and therefore $k$ is large; when the viscosity is small, the forces are distributed to a great distance and $k$ approaches 2 in the limit. This suggests the comparison

$$m = \infty \quad , \quad k = \infty$$

$$m = 2 \quad , \quad k = 2 \tag{18}$$

and further suggests as a first approximation

$$k \simeq m \tag{19}$$

It is then possible to replace $\tau$ by

$$\tau\left(\frac{1-M}{1-2M}\right) \tag{20}$$

With reference to the $\psi_1$ of Equation (11), it is possible to define the limiting angle of incline, $\psi_2'$, for the "secondary absolute stability" of a slope as

$$\psi_2' = \frac{1-2M}{1-M}\tan\psi_1 \tag{21}$$

If the slope angle, $\psi$ is less than $\psi_2'$, then the slope remains stable in spite of an arbitrarily large radius of fracture in the critical layer.

The $1/r$ dependence given by Equation (14) suggests that the increase in stress is finite even if the radius of the fracture line becomes infinite. However, if stress is propagated according to an exponential law, then the stress may diverge. This problem has not been solved for snow, although Bossinesq (see Kollbrunner) has worked on a similar theory for soils.

When the radius of the fracture line is small, the increase in stress is lower than the value given by Equation (16). It varies at first as $r_o^2$ and then approaches assymptotically a radius of the same order of magnitude as depth $y$.

The second extreme case, an extended horizontal fracture line, can be represented by a band of width $2X_o$ in the x-direction and infinitely long in the z-direction (see Fig. 2). For this case the increase in stress is

$$\Delta\tau = \frac{T'(K-2)}{X_o}\left(\frac{X_o}{x}\right)^{K-1} \tag{22}$$

where

$$T' = g X_0 \sin\psi = \tau X_0 \tag{23}$$

The change in stress at $X = X_0$ is

$$\Delta\tau = \tau(K-2) \tag{24}$$

and the total stress at $X = X_0$ is

$$\frac{\tau}{1-2M} \tag{25}$$

For this case, the steepest angle, $\psi_2''$ of "secondary absolute stability" is given by

$$\tan(\psi_2'')^2 = (1-2M)\tan\psi_1 \tag{26}$$

$\psi_2''$ is slightly smaller than $\psi_2'$ because the boundaries to which the stress is transferred is larger for the case of the cylinder.

In Fig. 8 the angles $\psi_1$, $\psi_2'$ and $\psi_2''$ are shown as functions of M for three values of the parameter $\omega$ .

The importance of the "compressibility factor," $M$ , can be observed. During settling and destructive metamorphism, M decreases, consequently, stability increases. However, if the critical layer is near the ground, constructive metamorphism tends to increase $M$ .

As mentioned at the beginning of this section, primary stability is a prerequisite for secondary stability: if the critical curve is reached, a local fracture can only increase the stress at the boundaries, amplify the instability, and cause the fracture to be propagated ad infinitum.

## 5. STABILITY WITH A CONCENTRATED FORCE ACTING ON THE SURFACE

Vertical forces may be applied to a slab by the pass of a skier. The stresses are distributed throughout the snow with a maximum stress approximately below the point of application. As with the original load, the vertical force can be resolved into a tangential and normal component. Assuming that the

critical layer is intact at the moment of application of the force, then, if the angle of the slope is less than $\psi_1$ , the concentrated force can be increased arbitrarily without leading to failure.

It is convenient to introduce a dimensionless force, $\mathcal{N}$ , defined by

$$\mathcal{N} = \frac{\mathcal{K}}{\pi y^2 g} \tag{27}$$

where $\mathcal{K}$ is the applied force and $\pi y^2 g$ represents the weight of a cylinder whose height and radius are equal to the depth, $y$ . Since $\tau_1$ increases linearly with $\mathcal{N}$ (Fig. 9), there is a value $\mathcal{N}_c$ which corresponds to $\tau_c$ (Point A). For a specific radius of fracture, $r_0$ , a curve can be constructed which passes through Point A. Consequently, the critical layer fails and the fracture is propagated up to a radius, $r_{01}$ . For a very large $r_0$ , the influence of K disappears in relation to the weight of the cylinder of snow. Graphically, this is represented by a horizontal line which intersects the former straight line at B with abcissa $\mathcal{N}_B$ and ordinate $\tau_{1\infty}$ . If $\tau_c$ is greater than $\tau_{1\infty}$ , and $\mathcal{K}$ is large enough to initiate a fracture, then A is to the right of B and the fracture propagates. The abcissa of B, $\mathcal{N}_B$ , is thus the maximum force that can be applied without inducing fracture propagation. As shown in Fig. 10, $\mathcal{N}$ is a function of the slope angle $\psi$ , the compressibility $M$ , and the parameter $w$ .

The angle $\psi_1$, exists for $0 < M < M_1$

$$M_1 = \frac{\sin w}{(1 + \sin w)} \tag{28}$$

If $\psi < \psi_1$ , no fracture can be produced and hence $\mathcal{N}_B$ does not exist; however, if $\psi > \psi_1$ , $\mathcal{N}_B$ exists and is greater than unity. For $M_1 < M < \frac{1}{2}$ , $\mathcal{N}_B$ always exists and is less than unity for slopes less than $20^\circ$. Thus, $\mathcal{K}$ is approximately $\pi y^2 g$ for absolute stability. If the horizontal fracture line is considered, as for example produced by an elongated ski track, a similar analysis can be made,

however, as a result of Equation (21) and (26), $\tan\psi$ must be replaced by $\frac{\tan\psi}{1-M}$.

## CONCLUSIONS

It seems that this study describes rather well the observed phenomona; however quantitative values cannot be attributed because the hypotheses which were used for their analytical simplicity are only approximations. It is likely that the introduction of the number $m$, and the derived $M$ which describe the plastic behavior of the snow, does not stray too far from reality. On the other hand, the hypotheses concerning the propagation of stress in the section on secondary stability should be received with more skepticism,- results from these hypotheses may entail a large factor of error. It must also be realized that it is difficult to procure experimental values of $\tau_c$, $w$, $m$ etc. Measurements made in the upper or lower portions of an avalanche zone do not necessarily describe the mean values in the critical layers of the slab prior to release. In order to compare theory with experiment, it is necessary to measure and average the parameters of the very slab which is about to release! The slab would also have to represent the theoretical conditions that were chosen in this study: large, constant slope, and free from natural anchors. In view of these difficulties, it seems that this study, inexact as it is, may already exceed what can be determined by experiment.

## REFERENCES

Haefeli, R. 1942 Schweizer archiv fur angewandte wissenschaft und technik, Heft 9-12

Kollbrunner, C. Fundation und Konsolidation, Bd. I.

FIGURES

Fig. 1 Distribution of the size of slab avalanches in the region of the Parsenn between 1959 and 1963.

Fig. 2 Reference of coordinate axes, stresses and angles.

Fig. 3 Mohr's plane, principal stresses and definition of $\tau_c$ .

Fig. 4 $\tau_1/g$ as a function of the angle of the slope for constant snow thickness.

Fig. 5 $\tau_1/g_0$ as a function of the angle of the slope for constant snow height.

Fig. 6 Maximum slope for primary absolute stability.

Fig. 7 $\tau_1/g \cos\psi$ as a function of the compressibility, M.

Fig. 8 Maximum slope for secondary absolute stability.

Fig. 9 Fracture line radius for a concentrated force.

Fig.10 Maximum concentrated force as a function of the slope angle for different values of the compressibility, M, at $\omega = 30^\circ$ .

Fig. 1

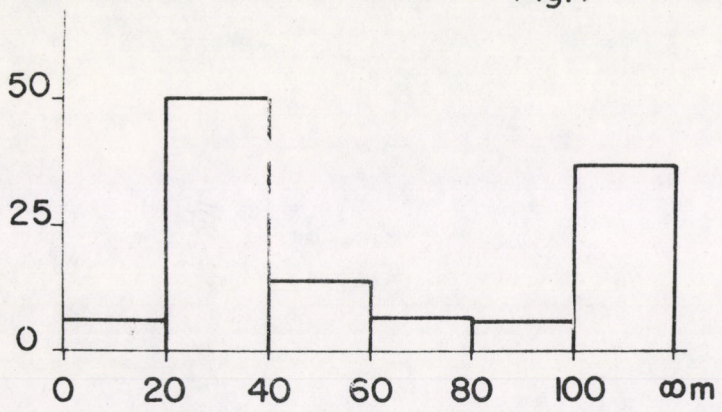


Fig. 2

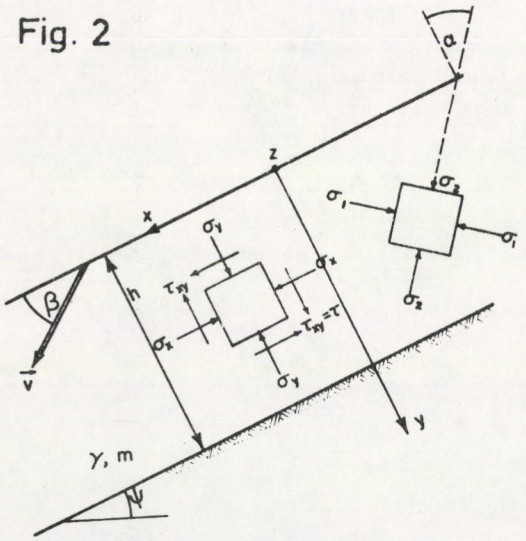


Fig. 3

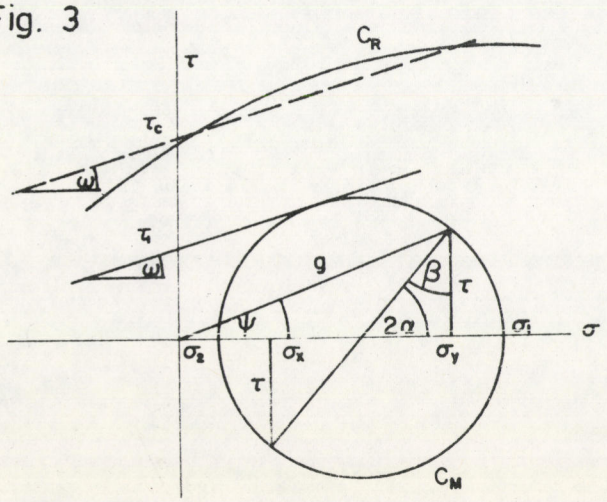


Fig. 4

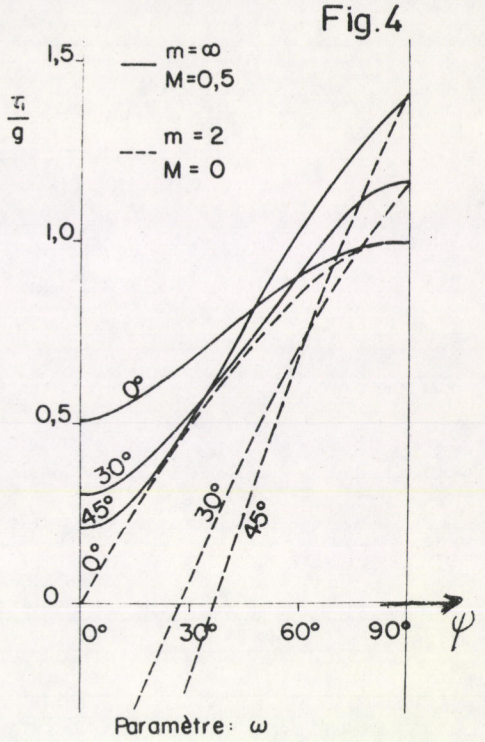


Fig. 5

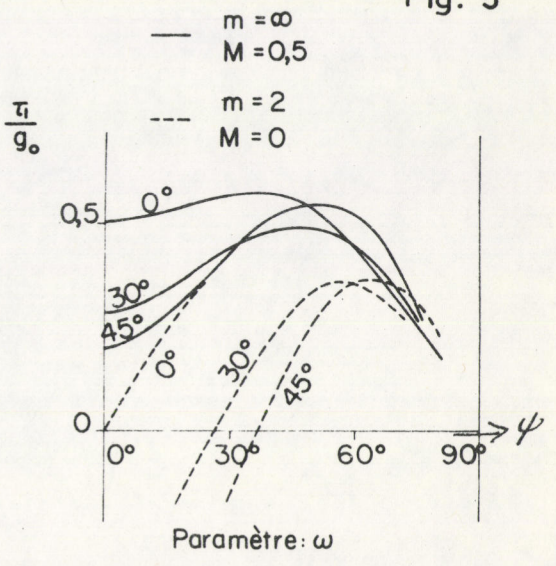

Fig. 6

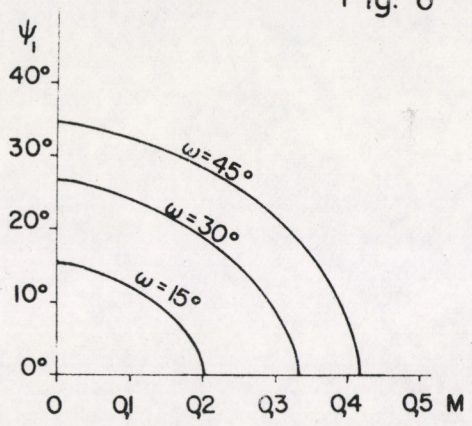


Fig. 9

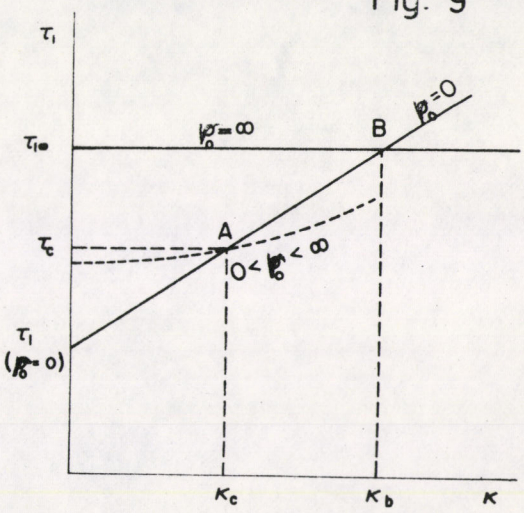


Fig. 7

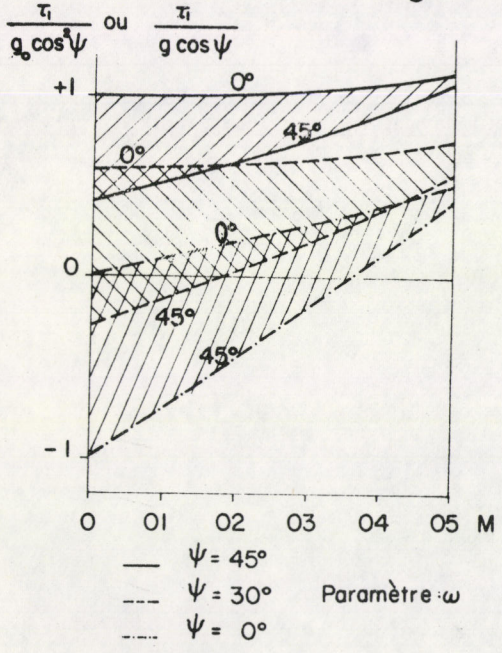


Fig. 8

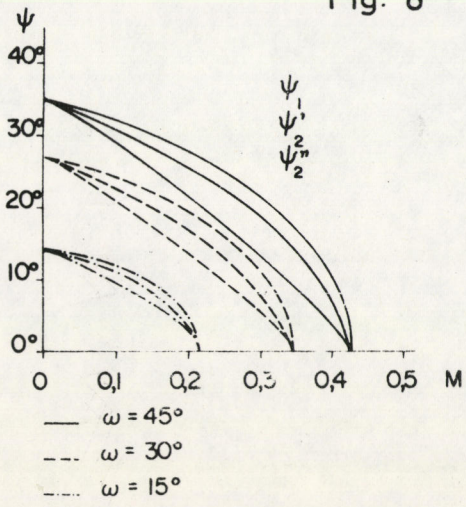


Fig. 10